Predicting stress intensity factor in pressurized cracked tubes using neural networks

Yassine EL KIRI [1*], *Ouassim* MEHDI BILLAH [1], *Zakaria* MIGHOUAR [1], *Laidi* ZAHIRI [1] and *Khalifa* MANSOURI [1]

[1]Laboratory of Modelling and Simulation of Intelligent Industrial Systems (M2S2I) ENSET, Hassan II University of Casablanca, Morocco

Abstract. Artificial intelligence is fundamentally reshaping how we approach complex engineering challenges, offering solutions that are both swift and remarkably accurate. In this paper, we detail the development of a predictive model, built upon neural networks, to estimate the stress intensity factor (K_I) in cracked tubes. By drawing upon a well-established analytical model, our aim was to devise a simple yet highly effective alternative to traditional numerical analyses. Thanks to strategic data augmentation, the model was meticulously refined and demonstrated exceptional accuracy. This study confirms AI's potential to provide reliable and rapid modeling in the critical field of fracture mechanics. Moreover, the explicit nature of the mathematical equation resulting from our neural network allows for direct and easy implementation in computer or mobile applications, thus facilitating its practical use in the field.

Keywords: Pipeline, pressure, crack, stress intensity factor, artificial neural network

1 Introduction

Ensuring the structural integrity of pressurized pipelines is of paramount importance for industries transporting fluids, particularly in the oil and gas sectors, where any failure can lead to catastrophic consequences for safety, the environment, and the economy [1-3]. These critical infrastructures are constantly subjected to high operational stresses, including the internal pressure of the fluids and various external loads such as corrosion, ground movement, or mechanical damage [1,4]. The presence of defects, such as cracks, poses a serious threat, potentially leading to unexpected ruptures well below the material's nominal strength [1-2]. Therefore, a rigorous crack assessment is indispensable to prevent these failures and guarantee the long-term reliability of pipelines [5].

Within this framework, fracture mechanics provides the necessary tools to characterize and analyze the behavior of cracked materials [6-7]. The stress intensity factor K_I (Mode I, or opening mode) is a fundamental parameter of this discipline, allowing quantification of

* Corresponding author: yassine.elkiri-etu@etu.univh2c.ma

the severity of the stress field at the tip of a crack in a loaded material [1,8,9]. Its value directly depends on the pipeline's geometry, the crack's size and location, as well as the magnitude of applied stresses, notably the internal pressure [1,3,7,9,10]. The importance of K_I lies in its ability to describe the driving force behind crack propagation: rapid growth and sudden fracture can occur if K_I exceeds the material's critical fracture toughness (K_{IC}) [8,9,11].

Evaluating K_I is crucial for anticipating crack growth due to fatigue, stress corrosion cracking, or other degradation mechanisms [7]. Numerical analysis methods, such as the Finite Element Method (FEM) and Extended Finite Element Method (XFEM), are commonly used to calculate K_I and assess the impact of defects on the remaining service life of pipelines [1,6,9,10,12]. These methods provide precise distributions of the stress intensity factor at the crack tip [12]. Industry standards, such as API 579-1/ASME FFS-1, integrate K_I evaluation into their Fitness-For-Service procedures [9,11,13]. These standards offer consensual methods for quantitatively assessing observed damage in in-service equipment and include evaluation techniques for crack-like flaws [9]. The "leak-before-break" approach, based on fracture mechanics and K_I evaluation, is also a central concept for demonstrating the integrity of pipeline and pressure vessel components, aiming to ensure that a leak is detected before an unstable fracture [7,14]. These analyses are essential for transitioning from a design approach based solely on stresses to one based on fracture mechanics, which is more realistic given the inevitable presence of defects [11].

To evaluate the impact of cracks on the mechanical strength of structures, we rely on fracture mechanics [15]. Semi-elliptical cracks, in particular, pose more complex problems than other types of defects. Figure 1 shows the typical shape of a semi-elliptical crack.

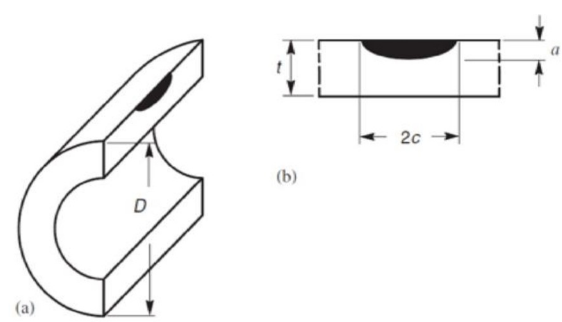

Fig. 1. (a) Tube with a semi-elliptical crack, (b) Crack geometry [16-17].

Since 2020, there has been a noticeable increase in research incorporating artificial intelligence [18-21] to tackle complex problems in physics and engineering. These approaches stand out due to their precise and rapid performance, which can even surpass what traditional numerical simulations offer.

However, an extensive search to date has not revealed any existing work predicting the stress intensity factor K_I using neural networks for pipelines with identical geometries, subjected solely to internal pressure, and featuring an external crack of a specific configuration. This observation highlights a gap in the literature for this precise defect assessment scenario, underscoring a significant opportunity for future research in artificial intelligence applied to fracture mechanics.

In this paper, we build upon the findings of a theoretical model concerning a cracked pressure pipe. Our objective is to construct a model capable of predicting the stress intensity factor. To achieve this, we will develop this model using Machine Learning, specifically through the application of artificial neural networks.

Nomenclature:
σ_{nom}: Nominal stress applied to the structure
E_k : Elliptical factor which takes into account the shape of the crack
M_F: Form factor related to the overall geometry of the structure
M_{TM}: Correction factor for tube wall thickness
a: Crack depth
c: Half-length of surface crack
t: Pipeline wall thickness
s: Exponent that adjusts the dependence between crack depth and thickness

2 Materials and methods

2.1 Theoretical model

The stress intensity factor ($K_{I,ANA}$) is a fundamental parameter in fracture mechanics. It enables us to quantify the severity of stresses at a crack tip and, by extension, to assess its potential for propagation. This factor is calculated specifically for semi-elliptical longitudinal cracks found in the base metal (away from welds) of an internally pressurized pipeline. The calculation meticulously accounts for the complex interplay between the defect's shape and the applied stresses, as laid out in Equation 1. This formula originates from analytical models that are well-established benchmarks within the field of fracture mechanics. Indeed, the equation itself integrates various terms to precisely describe both the crack and the structure's geometry, alongside the external loading conditions [10-11].

$$K_{I,ANA} = \left[M_F + (E_K\sqrt{\frac{c}{a}} - M_F)\left(\frac{a}{t}\right)^s\right]\frac{\sigma_{nom}\sqrt{\pi a}}{E_K}M_{TM} \tag{1}$$

2.2 Predictive model

Our predictive model was designed by leveraging the established results of the analytical model [12]. This provided us with a comprehensive collection of input-output data, simulating crack propagation in pressurized tubes. The core idea is to offer an alternative method for evaluating the stress intensity factor, significantly simplifying the process and sidestepping the need for the extensive expertise in finite element analysis often demanded by numerical methods. The accompanying flowchart illustrates the algorithmic logic of a Python script, implemented with the PyTorch library and executed within the Google Colab computing environment.

The implementation of our Machine Learning approach unfolded in four distinct stages. The first, Data Preparation, involved loading, augmenting, splitting, and normalizing the data to make it ready for use. Next, the second phase, Architecture Justification, entailed an experimental approach to determine the ideal number of neurons. For this, we tested various configurations and selected the one that yielded the best results on the test set, a decision supported by a justification graph. The third phase, Final Model Training, focused on intensively training the chosen architecture, with its progress monitored via a loss curve. Finally, the fourth and last stage, Final Evaluation and Results, allowed us to use the trained model to make predictions, calculate essential performance indicators such as RMSE and percentage error, and present our conclusions through a comparative table and a model topology diagram. This complete process is further illustrated in Figure 2.

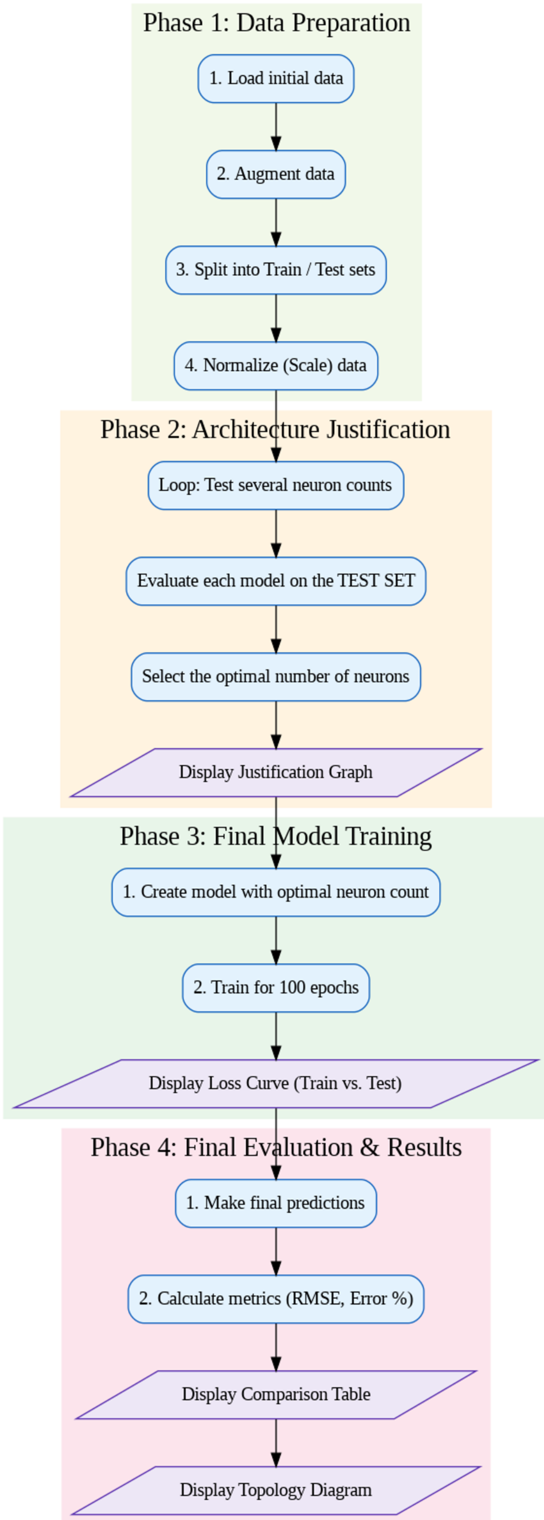

Fig.2. Script execution process diagram.

Figure 3 illustrates our approach to selecting the optimal neural network architecture. It shows how we evaluated the performance of various models based on their complexity (represented by the number of neurons in the hidden layer on the horizontal axis) and their final error (MSE) on the test set (on the vertical axis).

We observed a clear improvement as complexity increased, with the error curve dropping sharply between 4 and 8 neurons. An acceptable performance threshold was established at an MSE of 0.006, which is indicated on the graph by the dotted green line. The 8-neuron model proved to be the first, and therefore the simplest, to achieve this level. Although more complex architectures (with 12, 16, 24, or 32 neurons) achieved marginally better performance, the improvement was minimal. Consequently, in adherence to the principle of simplicity (Occam's Razor), we selected the 8-neuron option (marked by the dashed red line), as it represents the best compromise between model simplicity and reaching the required performance level.

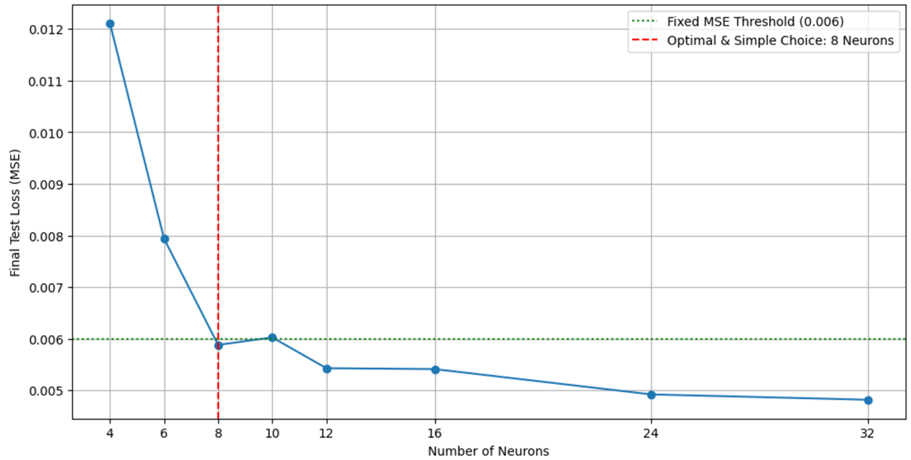

Fig.3. Model performance vs number of neurons in hidden layer.

Figure 4 allows us to track the performance evolution of our final model throughout its 100 training epochs. It highlights two crucial indicators: the Training Loss, which reflects the model's error on the data it has already processed, and the Test Loss, which gauges its effectiveness on entirely new and unseen data.

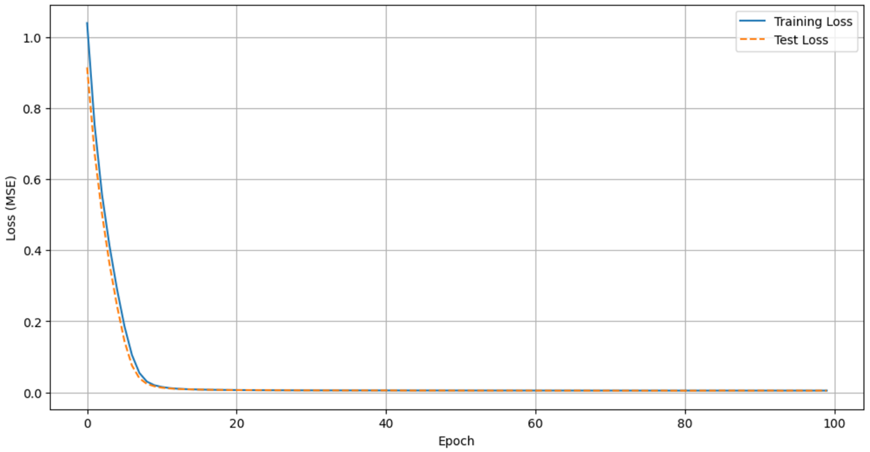

Fig.4. Evolution of MSE loss during training.

What we observe is a convergence that is both rapid and remarkably stable. Both curves decline significantly within the first 20 epochs, demonstrating the model's swift assimilation of the data's underlying structure. Subsequently, they stabilize, converging towards an extremely low, near-zero errors. The close alignment of the Test Loss curve (dashed orange) with the Training Loss curve is an excellent sign: it means our model generalizes effectively and avoids the pitfall of overfitting. Ultimately, this graph confirms the quality and robustness of our training process.

Figure 5 illustrates our data augmentation methodology: a controlled simulation designed to expand an initially limited dataset. This process runs for 2000 iterations. In each round, one of the twelve original data rows is randomly chosen to serve as a template. Subsequently, a slight random 'noise' generated using a normal distribution for enhanced realism is added to each of its values (a, c, p, and $K_{I,ANA}$), thereby creating a new synthetic data point.

A crucial validation step then takes place: our script checks the physical plausibility of this new point, specifically ensuring that all its values remain positive. If the point is deemed valid, it is added to our new dataset; otherwise, it is simply discarded. This approach enables us to transform a small number of reliable samples into a vast volume of synthetic data, significantly bolstering the robustness of our artificial intelligence model's training.

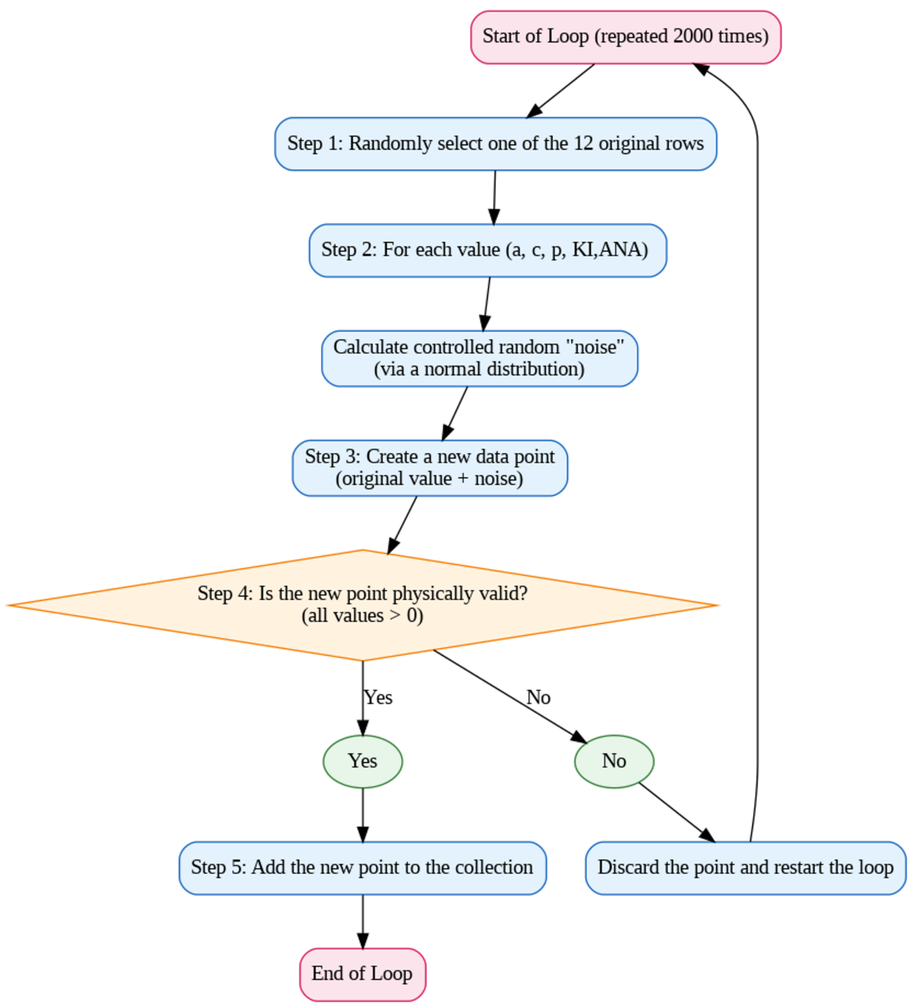

Fig.5. Diagram of the data point augmentation process.

The architecture of a simple feedforward neural network, which is commonly used for regression tasks, is built in several layers. It all begins with an input layer, designed to receive three specific features. This data is then transmitted and processed by a hidden layer of eight neurons. This is where a Rectified Linear Unit (ReLU) activation function comes into play, critically introducing non-linearity. This allows the model to grasp complex relationships that go beyond simple linear trends. After this processing, the information consolidated by this hidden layer then feeds into the output layer, which consists of just a single neuron. The final step employs a linear function, ensuring that the model's ultimate numerical prediction remains unconstrained. This entire architecture is clearly illustrated in Figure 6.

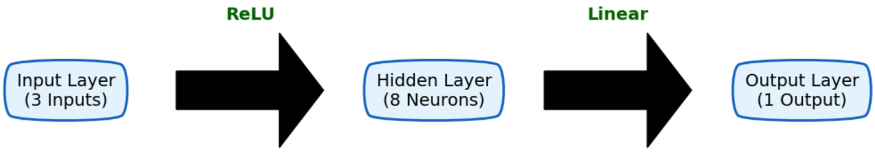

Fig.6. Topology of the optimized model.

3 Results and discussions

3.1 Predictive stress intensity factor

We evaluated the accuracy of our artificial intelligence-based predictive model ($K_{I,PRED}$) by directly comparing it with the theoretical reference solution ($K_{I,ANA}$). The results of this analysis clearly highlighted the exceptional reliability of our model. Most prediction errors proved to be minimal, with many even falling below 1%, and some reaching as little as 0.01% in several cases, which demonstrates excellent concordance with the theoretical values. All the details of this comparison are presented in Table 1.

Table 1. Results of the predictive model.

a (mm)	c (mm)	p (MPa)	$K_{I,ANA}$ (MPa.m$^{0.5}$) [12]	$K_{I,PRED}$ (MPa.m$^{0.5}$)
2,75	4,6	5,9	3,604	3,383
		14,76	9,015	9,522
		29,52	18,03	18,188
	6,875	5,9	4,585	4,853
		14,76	11,47	10,992
		29,52	22,939	23,073
6,85	11,41	5,9	6,385	6,349
		14,76	15,974	15,768
		29,52	31,947	32,062
	17,125	5,9	9,147	9,124

	14,76	22,883	22,733
	29,52	45,767	45,771

Looking at this table, it's clear our model does a very respectable job at predicting the stress intensity factor (K_I). The values it generates ($K_{I,PRED}$) are generally very close to the analytical reference values ($K_{I,ANA}$), which speaks volumes about its robustness.

We do, however, observe a few nuances:

- For the initial configurations (small crack a = 2.75 mm, c = 4.60 mm), the model shows a slight tendency to overestimate K_I.
- Conversely, for the same small a but a slightly deeper c (6.875 mm), it tends to underpredict it somewhat.
- The most striking agreement is seen with medium-sized cracks (a = 6.85 mm, c = 11.41 mm); here, the predictions are almost perfect, remarkably faithful to the analytical values.
- Finally, for larger and very deep cracks (a = 6.85 mm, c = 17.125 mm), the model underpredicts K_I a bit more noticeably.

All in all, while minor discrepancies might pop up at the extremes or in specific configurations, the model does an admirable job of capturing the general trends. It delivers highly reliable predictions, confirming its potential as a practical tool.

3.2 Precision performance

The impact of data augmentation on the predictive model's performance is nothing short of spectacular. Without this enhancement, the model yielded an RMSE of 7.4769 MPa.$m^{0.5}$, a performance we considered mediocre. However, incorporating data augmentation completely transformed the model: its RMSE then plummeted to just 0.2464 MPa.$m^{0.5}$. This represents a colossal improvement, equating to a reduction of over 95% in the RMSE. All the details of this comparison can be found in table 2.

Table 2. Precision metrics

Dataset	**RMSE**
Without augmentation	7.4769 MPa.$m^{0.5}$
Data Augmentation	0.2464 MPa.$m^{0.5}$

3.3 Prediction equation

Our prediction equation unfolds in two distinct steps. First, the three input values (a, c, p) are linearly combined using a weight matrix and a bias vector. This process allows us to generate eight intermediate values (denoted h_1 to h_8), as detailed in Equation 2. Subsequently, the ReLU activation function is applied to each of these eight values. Finally, the ultimate prediction ($K_{I,\ PRED}$) is calculated by performing a weighted sum of these eight activated outputs, with a final bias added, in accordance with Equation 3. This direct mathematical formulation of the neural network is a significant advantage, as it facilitates easy and rapid implementation in computer or mobile applications, thereby offering a practical tool for decentralized K_I factor calculation in the field.

$$\begin{pmatrix} h_1 \\ h_2 \\ h_3 \\ h_4 \\ h_5 \\ h_6 \\ h_7 \\ h_8 \end{pmatrix} = \begin{pmatrix} 0.560 & 0.569 & 0.664 \\ -0.192 & -0.807 & -0.401 \\ 0.136 & -0.447 & 0.183 \\ 0.375 & -0.331 & 0.473 \\ 0.051 & 0.091 & -0.483 \\ -0.275 & 0.565 & 0.757 \\ -0.017 & 0.405 & -0.944 \\ -0.401 & -0.177 & -0.160 \end{pmatrix} \begin{pmatrix} a \\ c \\ p \end{pmatrix} + \begin{pmatrix} -0.005 \\ 0.168 \\ 0.206 \\ -0.519 \\ 0.419 \\ 0.199 \\ 0.602 \\ 0.490 \end{pmatrix} \quad (2)$$

$$K_{I,PRED} = f\left(\begin{pmatrix} 0.583 & -0.364 & -0.333 & -0.563 & -0.443 & 0.523 & -0.292 & 0.164 \end{pmatrix} \begin{pmatrix} f(h_1) \\ f(h_2) \\ f(h_3) \\ f(h_4) \\ f(h_5) \\ f(h_6) \\ f(h_7) \\ f(h_8) \end{pmatrix} + 0.137 \right) \quad (3)$$

4 Conclusions

This work clearly highlighted the effectiveness of a novel AI-driven predictive approach for estimating the stress intensity factor (K_I) in cracked tubes. Thanks to a judicious application of data augmentation, our neural network was finely tuned. The final 8-neuron architecture was selected as it represented the simplest choice to achieve a test loss below our predefined performance threshold of 0.006 (MSE). This model subsequently exhibited remarkable precision, registering an RMSE of 0.2464 MPa.m$^{0.5}$. In summary, this study confirms AI's capability to reliably model complex fracture mechanics phenomena, thereby offering a fast and accurate alternative to traditional simulations. Moreover, the explicit nature of the mathematical equation resulting from our neural network allows for direct and easy implementation in computer or mobile applications, thus facilitating its practical use in the field.

References

[1] K. Yakoubi, S. Montassir, H. Moustabchir, A. Elkhalfi, M. L. Scutaru, and S. Vlase, “T-Stress Evaluation Based Cracking of Pipes Using an Extended Isogeometric Analysis (X-IGA). Symmetry 2022, 14, 1065,” 2022, s Note: MDPI stays neutral with regard to jurisdictional claims in published.

[2] B. Mechab, A. Benouar, B. A. B. Bouiadjra, M. Salem, and K. Kaddouri, “A New Investigation of Plastic Limit of Repaired Steel Pipe Elbow With Bonded Composite Wrap Subjected to Internal Pressure,” J. Press. Vessel Technol., vol. 147, no. 6, p. 61302, 2025.

[3] Z. Li, X. Jiang, and H. Hopman, “Surface crack growth in offshore metallic pipes under cyclic loads: A literature review,” J. Mar. Sci. Eng., vol. 8, no. 5, p. 339, 2020.

[4] M. Ali Ghaffari and H. Hosseini-Toudeshky, “Fatigue crack propagation analysis of repaired pipes with composite patch under cyclic pressure,” J. Press. Vessel Technol., vol. 135, no. 3, p. 31402, 2013.

[5] Ľ. Gajdoš, M. Šperl, J. Bayer, and J. Kuželka, “Comparison of J Integral Assessments for Cracked Plates and Pipes,” Materials (Basel)., vol. 14, no. 15, p. 4324, 2021.

[6] S. Montassir, K. Yakoubi, H. Moustabchir, A. Elkhalfi, D. K. Rajak, and C. I. Pruncu, “Analysis of crack behaviour in pipeline system using FAD diagram based on numerical simulation under XFEM,” Appl. Sci., vol. 10, no. 17, p. 6129, 2020.

[7] Y. Choi and S.-J. Lee, “Probabilistic Fatigue Crack Growth Prediction for Pipelines

with Initial Flaws," Buildings, vol. 14, no. 6, p. 1775, 2024.

[8] S. El Fakkoussi, S. Vlase, M. Marin, O. Koubaiti, A. Elkhalfi, and H. Moustabchir, "Predicting Stress Intensity Factor for Aluminum 6062 T6 Material in L-Shaped Lower Control Arm (LCA) Design Using Extended Finite Element Analysis," Materials (Basel)., vol. 17, no. 1, p. 206, 2023.

[9] P. Seenuan, N. Noraphaiphipaksa, and C. Kanchanomai, "Stress Intensity Factors for Pressurized Pipes with an Internal Crack: The Prediction Model Based on an Artificial Neural Network," Appl. Sci., vol. 13, no. 20, p. 11446, 2023.

[10] W. Wang, A. Zhou, G. Fu, C.-Q. Li, D. Robert, and M. Mahmoodian, "Evaluation of stress intensity factor for cast iron pipes with sharp corrosion pits," Eng. Fail. Anal., vol. 81, pp. 254–269, 2017.

[11] Z. Chaplin, "Major accident hazard pipeline failure frequency calculation using fracture mechanics," in Safety and Reliability, Taylor & Francis, 2017, pp. 217–232.

[12] K. Yakoubi et al., "An extended finite element method (XFEM) study on the elastic t-stress evaluations for a notch in a pipe steel exposed to internal pressure," Mathematics, vol. 9, no. 5, p. 507, 2021.

[13] S. Kalyanam et al., "Constraint effects in slow crack growth test methods for service life prediction of high density polyethylene piping," J. Press. Vessel Technol., vol. 142, no. 4, p. 41508, 2020.

[14] D. J. Shim, J. S. Park, R. Kurth, and D. Rudland, "Surface to through-wall crack transition model for circumferential cracks in pipes," J. Press. Vessel Technol., vol. 144, no. 1, p. 11306, 2022.

[15] T. L. Anderson and T. L. Anderson, Fracture mechanics: fundamentals and applications. CRC press, 2005.

[16] S. Cravero and C. Ruggieri, "Structural integrity analysis of axially cracked pipelines using conventional and constraint-modified failure assessment diagrams," Int. J. Press. Vessel. Pip., vol. 83, no. 8, pp. 607–617, 2006.

[17] F. Dotta and C. Ruggieri, "Structural integrity assessments of high pressure pipelines with axial flaws using a micromechanics model," Int. J. Press. Vessel. Pip., vol. 81, no. 9, pp. 761–770, 2004.

[18] M. Lo, S. Karuppanan, and M. Ovinis, "ANN-and FEA-based assessment equation for a corroded pipeline with a single corrosion defect," J. Mar. Sci. Eng., vol. 10, no. 4, p. 476, 2022.

[19] Y. El Kiri, L. Zahiri, K. Mansouri, Z. Mighouar, and S. El Ouardi, "Prediction of the rupture pressure of a corroded pipeline by ANN," in E3S Web of Conferences, EDP Sciences, 2023, p. 31.

[20] Y. El Kiri, Z. Mighouar, L. Zahiri, K. Mansouri, S. El Ouardi, and H. Chaiti, "Predicting the failure of plain dent pipeline subjected to cyclic loads using an artificial neural network," in 2023 7th IEEE Congress on Information Science and Technology (CiSt), IEEE, 2023, pp. 179–186.

[21] D. Oh, J. Race, S. Oterkus, and B. Koo, "Burst pressure prediction of API 5L X-grade dented pipelines using deep neural network," J. Mar. Sci. Eng., vol. 8, no. 10, p. 766, 2020.

[22] J. C. Newman Jr, "Fracture analysis of surface-and through-cracked sheets and plates," Eng. Fract. Mech., vol. 5, no. 3, pp. 667–689, 1973.

[23] M. El-Sayed, A. El Domiaty, and A. H. I. Mourad, "Fracture assessment of axial crack in steel pipe under internal pressure," Procedia Eng., vol. 130, pp. 1273–1287, 2015.

[24] L. Zahiri, Z. Mighouar, H. Khatib, K. Mansouri, and B. Salhi, "Fatigue behavior of longitudinal welded pipes subjected to cyclic internal pressure, containing welding defects," Int. J. Mech. Eng. Technol., pp. 560–569, 2018.